



Plastid ribosome protein L5 is essential for post-globular embryo development in *Arabidopsis thaliana*

Gilles Dupouy¹ · Emma McDermott¹ · Ronan Cashell¹ · Anna Scian¹ · Marcus McHale¹ · Peter Ryder¹ · Joelle de Groot¹ · Noel Lucca¹ · Galina Brychkova¹ · Peter C. McKeown¹ · Charles Spillane¹

Received: 17 October 2021 / Accepted: 14 February 2022 / Published online: 5 March 2022
© The Author(s) 2022

Abstract

Plastid ribosomal proteins (PRPs) can play essential roles in plastid ribosome functioning that affect plant function and development. However, the roles of many PRPs remain unknown, including elucidation of which PRPs are essential or display redundancy. Here, we report that the nuclear-encoded PLASTID RIBOSOMAL PROTEIN L5 (PRPL5) is essential for early embryo development in *A. thaliana*, as homozygous loss-of-function mutations in the *PRPL5* gene impairs chloroplast development and leads to embryo failure to develop past the globular stage. We confirmed the *prpl5* embryo-lethal phenotype by generating a mutant CRISPR/Cas9 line and by genetic complementation. As *PRPL5* underwent transfer to the nuclear genome early in the evolution of Embryophyta, PRPL5 can be expected to have acquired a chloroplast transit peptide. We identify and validate the presence of an N-terminal chloroplast transit peptide, but unexpectedly also confirm the presence of a conserved and functional Nuclear Localization Signal on the protein C-terminal end. This study highlights the fundamental role of the plastid translation machinery during the early stages of embryo development in plants and raises the possibility of additional roles of plastid ribosomal proteins in the nucleus.

Keywords Plastid · Ribosome · Localization · Embryo development · *Arabidopsis thaliana*

Introduction

The plastid is an essential organelle in plant cells acquired through a unique endosymbiosis event in the common ancestor of all Archaeplastida, including green plants (Viridiplantae), in which a non-plastid eukaryote absorbed a photosynthetic bacterium (Kishino et al. 1990; Moreira et al. 2000; Stiller 2007; Nowack and Weber 2018). Gene transfer processes have occurred between the original plastid genome (of prokaryote origin) and the nuclear genome during the evolution of the photosynthetic eukaryotic cell leading most plastid-derived genes to relocate to the nucleus (Martin et al. 2002; McFadden 2014). This transfer is thought to have

happened in parallel with the transfer of mitochondrial genes to the nucleus following the endosymbiosis event underlying eukaryotes. Since transferred genes include many of those responsible for the fundamental cellular and metabolic functions of the plastid their protein products needs to be targeted back to plastids by anterograde signaling to ensure their function (Bräutigam et al. 2007). Approximately two thirds of the Plastid Ribosomal Protein (PRPs) genes in the model eudicot *Arabidopsis thaliana* have been transferred from the plastid to the nucleus. Most of these genes have also been lost from the plastid genome with a small proportion still remaining and, thus, potentially redundant with their nuclear duplicates (Allen 2018).

Many prokaryote ribosomal proteins (RPs) have been shown to be essential in *E. coli* (Shoji et al. 2011), mostly being homologs of cyanobacteria-derived plastid RPs (Yamaguchi and Subramanian 2000). Similarly, many cyanobacteria-derived RPs have also been reported as essential for embryo development in at least one Embryophyta species (Table 1). Most essential PRPs are reported as necessary for embryogenesis in *A. thaliana* correlating with the essential functions of plastids in cellular metabolism before the

Communicated by Weicai Yang .

✉ Charles Spillane
charles.spillane@nuigalway.ie

¹ Genetics and Biotechnology Lab, Plant and AgriBiosciences Research Centre (PABC), Ryan Institute, Aras de Brun, National University of Ireland Galway, University Road, Galway H91 REW4, Ireland

Table 1 Plastid ribosome subunits in *A.thaliana* and functional homologs in *E.coli*

PRP	Essentiality in <i>E. coli</i> (Shoji et al. 2011)	<i>A. thaliana</i> Locus ID	Essentiality post Globular Stage in <i>A. thaliana</i>	Reference (<i>A. thaliana</i>)
S1	Essential	AT5G30510	Non-essential	Romani et al. (2012)
S2	Essential	ATCG00160	Essential	Rogalski et al. (2008)
S3	Essential	ATCG00800	Essential	Fleischmann et al. (2011)
S4	Essential	ATCG00380	Essential	Rogalski et al. (2008)
S5	Essential	AT2G33800	Essential	Bryant et al. (2011); Muralla et al. (2011); Lloyd and Meinke (2012)
S7	Essential	ATCG00900/ ATCG01240	NA	NA
S8	Essential	ATCG00770	NA	NA
S9	Non-essential	AT1G74970	Essential	Hsu et al. (2010); Lloyd and Meinke (2012)
S10	Essential	AT3G13120	NA	NA
S11	Essential	ATCG00750	Essential	Muralla et al. (2011); Lloyd and Meinke (2012)
S12	Essential	ATCG00065/ ATCG01230	Putative essential	Asakura and Barkan (2006)
S13	Essential	AT5G14320	Essential	Bryant et al. (2011); Lloyd and Meinke (2012)
S14	Essential	ATCG00330	Essential	Jiang et al. (2018)
S15	NA	ATCG01120	Non-essential	Fleischmann et al. (2011)
S16	Essential	ATCG00050	Essential	Fleischmann et al. (2011)
S17	Non-essential	AT1G79850	Non-essential	Woo et al. 2002; Romani et al. (2012); Lloyd and Meinke (2012)
S18	Essential	ATCG00650	Essential	Rogalski et al. (2006)
S19	Essential	ATCG00820	NA	NA
S20	NA	AT3G15190	Essential	Romani et al. (2012)
S21	NA	AT3G27160	Non-essential	Morita-Yamamuro et al. (2004)
L1	NA	AT3G63490	Essential	Bryant et al. (2011); Romani et al. (2012); Lloyd and Meinke (2012)
L2	Essential	ATCG00830/ ATCG01310	NA	NA
L3	Essential	AT2G43030	NA	NA
L4	Essential	AT1G07320	Essential	Muralla et al. (2011); Lloyd and Meinke (2012)
L5	Essential	AT4G01310	Essential	This Study
L6	Essential	AT1G05190	Essential	Hsu et al. (2010); Muralla et al. (2011); Lloyd and Meinke (2012)
L7	Essential	NA	NA	NA
L9	NA	AT3G44890	NA	NA
L10	Essential	AT5G13510	Essential	Bryant et al. (2011); Lloyd and Meinke (2012)
L11	NA	AT1G32990	Non-essential	Pesaresi et al. 2006; Lloyd and Meinke (2012)
L12	Essential	AT3G27850	NA	NA
L13	Essential	AT1G78630	Essential	Hsu et al. (2010); Muralla et al. (2011); Lloyd and Meinke (2012)
L14	Essential	ATCG00780	NA	NA
L15	Non-essential	AT3G25920	Essential	Bobik et al. (2018)
L16	Essential	ATCG00790	NA	NA
L17	Essential	AT3G54210	NA	NA
L18	Essential	AT1G48350	Essential	Bryant et al. (2011); Lloyd and Meinke (2012)
L19	Essential	NA	NA	NA

Table 1 (continued)

PRP	Essentiality in <i>E. coli</i> (Shoji et al. 2011)	<i>A. thaliana</i> Locus ID	Essentiality post Globular Stage in <i>A. thaliana</i>	Reference (<i>A. thaliana</i>)
L20	Essential	ATCG00660	Essential	Rogalski et al. (2008)
L21	Non-essential	AT1G35680	Essential	Yin et al. (2012)
L22	Essential	ATCG00810	Essential	Fleischmann et al. (2011)
L23	Essential	ATCG01300/ ATCG00840	Essential	Fleischmann et al. (2011)
L24	Non-essential	AT5G54600	Non-essential	Nadine et al. (2012); Romani et al. (2012)
L25	NA	NA	NA	NA
L27	Non-essential	AT5G40950	Essential	Romani et al. (2012)
L28	Essential	AT2G33450	Essential for greening process and post germination	Romani et al. (2012)
L29	Non-essential	AT5G65220	NA	NA
L30	Non-essential	NA	NA	NA
L31	NA	AT1G75350	Essential	Hsu et al. (2010); Lloyd and Meinke (2012)
L32	NA	ATCG01020	Essential	Fleischmann et al. (2011)
L33	NA	ATCG00640	Non-essential but affects growth in response to cold stress	Rogalski et al. (2008)
L34	Non-essential	AT1G29070	NA	NA
L35	NA	AT2G24090	Essential	Romani et al. (2012)
L36	NA	ATCG00760/ AT5G20180	Non-essential	Fleischmann et al. (2011)

Overview of experimentally demonstrated essentiality of Plastid Ribosomal Proteins (PRPs) for embryogenesis and cell survival in *A. thaliana*. The essentiality of plastid ribosomal proteins encoded in the plastid genome has also been demonstrated in *N. tabacum*. Each PRP is compared to its homologous ribosomal protein (RP) in the cyanobacteria-related species *E. coli*. The essentiality of RPs for cell survival in *E. coli* has been assessed by Shoji et al. (2011). NA not available (no data)

start of photosynthetic activity, notably in lipid and starch biosynthesis (Neuhaus and Emes 2000). Genetic knockouts of these PRPs typically do not allow the embryo to develop further than the globular stage. This mutant phenotype highlights the necessity of the plastid translation mechanism as early as the globular stage of embryo development, and not before, even with the maternal-to-zygote transition occurring as early as the zygote (Zhao et al. 2019).

Some nuclear-encoded PRPs have been investigated in *A. thaliana* using genetic knockouts. PRPs in which loss-of-function mutations have been shown to lead to seed abortion have been considered as essential for embryo development and are summarized in Table 1. The essential requirement (essentiality) for plastid-encoded PRPs has been shown via knockout alleles in *Nicotiana tabacum* plastid genomes (biolistic chloroplast transformation) and considered essential based on leaf necrosis phenotypes. Among these *PRPS12* is putatively considered likely to be embryo lethal since the splicing of its mRNA is affected by the knockout of the gene *AtCAF2* (Asakura and Barkan 2006), but its essentiality for embryo development has not been directly demonstrated to date.

Notably, not all PRPs are reported to be essential for plant development including *PRPS1*, -S17, -L24 and -L28. Knockouts of *PRPS17* and *PRPL24* suggest they are non-essential. However *prps1-1* is shown to be only a knockdown

so it could be considered that the viability of *prps1-1* seeds could be due to leaky expression in the mutant line which allows embryo development. Despite being non-essential for embryogenesis, *PRPL28*, however, appears to be required for seed greening at later stages of embryogenesis since its knockout creates albino seeds which are able to germinate but subsequently die quickly (Romani et al. 2012). A knockout of *PRPS17* has been shown to reduce growth rate as well as leaf chlorophyll pigment (Woo et al. 2002). *PRPL24* (Nadine et al. 2012), *PRPS21* and *PRPL11* knockouts also lead to decreased plant size and reduced photosynthetic activity due to a decrease in the translational activity in plastids (Morita-Yamamuro et al. 2004; Pesaresi et al. 2006). *PRPL33* was reported to be required only in cold-stress conditions (Rogalski et al. 2008), and *PRPS15* and *PRPL36* for full photosynthetic activity (Fleischmann et al. 2011).

Some homologs of the essential RPs in *E. coli*, however, still remain to be verified in green plants (*PRPS2*, -S4, -S7, -S8, -S10, -S11, -S12, -S19, -L2, -L3, -L16, -L17, -L19). However, non-essentiality in *E. coli* may not necessarily translate to non-essentiality in green plants. For example, while its homolog in *E. coli* was shown as non-essential, *PRPL15* was revealed to be essential for embryo development in *A. thaliana* (Bobik et al. 2018).

In this study, we demonstrate that *PRPL5* is required for post-globular stage embryo development in *A. thaliana*

and we characterize the activity its N-terminal Chloroplast transit peptide (cTP) and C-terminal Nuclear localisation signal (NLS) which are completely absent from Chlorophyta and Charophyta homologous proteins.

Materials and methods

Plant material and genomic samples

Arabidopsis thaliana seeds were surface sterilized with Chlorine gas (3:1 bleach:hydrochloric acid in a bell jar for one hour). Seeds were germinated on 0.5 × Murashige and Skoog (MS) medium (Murashige and Skoog 1962) containing 1% w/v sucrose and 0.8% w/v agar, and grown in a Percival Tissue Culture cabinet under a 16:8 h light: dark (21 °C/18 °C) regime (Boyes et al. 2001) until they were transferred to soil (five parts Westland compost [Dunannon, N. Ireland]: 1 part perlite: 1 part vermiculite). Plants were grown in chambers under fluorescent lamps at 200 μmol m⁻² s⁻¹ with the same photoperiod.

Plant DNA extraction

Plant genomic DNA was extracted using 20 mg of rosette leaf which was grinded with glass beads and incubated in DNA extraction buffer [200 mM of Tris-HCl pH 7.5, 250 mM of NaCl, 25 mM of EDTA, 0.5% w/v of SDS] for 10 min at 60 °C. Samples were next mixed with equal volumes of ice cold isopropanol (1:1) and DNA was precipitated at –20 °C for 10 min followed by a centrifugation. Precipitated DNA was washed once with 70% ethanol, left over to dry, re-suspended in water and incubated at 60 °C for 10 min. To genotype plants, as wild type, heterozygous or homozygous, two different pairs of primers were used to span the insertion/removal site of the mutant alleles. The forward primer 5'-ATCCTCTCGAGGTAA GCGGT-3' and reverse primer 5'-TCTTCTCAGGTCGGT GTGGA-3' were used to span the T-DNA insertion from *prpl5-1* mutant allele, with the use of an additional internal reverse primer Lbb1.3 5'-ATTTTGCCGATTTTCGGAA C-3' to detect the presence of the T-DNA sequence. The forward primer 5'-CACGCGCTAGCTTTTCACG-3' and reverse primer 5'-AGGGGCTAAACGGAAAACCTCC-3' were used to span the Cas9-induced 1057 bp removal from *prpl5-2* mutant allele. In addition to the detection of a band of different size between wild-type and mutant alleles (1660 bp for WT and 603 bp for *prpl5-2*), one additional reverse primer 5'-TCCAAGGTGTGAGTCCCAGT-3' was used to detect the presence of the removed section from the wild-type allele.

RNA extraction and PRPL5 expression analysis

RNA extraction was performed on 20 mg rosette leaf tissue using the ISOLATE II RNA Plant kit (Bioline, UK). DNase treatment was performed on 1 μg of crude RNA using the DNase I amplification grade kit (Invitrogen, UK), and cDNAs were generated using the Superscript III First Strand Synthesis kit (Invitrogen, UK), following protocol supplied by the manufacturer. *PRPL5* expression was evaluated by RT-PCR using forward 5'-TGGGTTTAATCAACAACG AACGC-3' and reverse 5'- TCCAAACCCTTGTCGTTG TG -3' primers and RT-qPCR using forward 5'-TCAACG CCTCAAACCCTGTT-3' and reverse 5'-TCCAAACCCTTG TCGTTCTG-3' primers. *PRPL5* Expression was normalized with *EF-1α* (Wang et al. 2014) using forward 5'-TCACCC TTGGTGTCAAGCAGAT-3' and reverse 5'-CAGGGTTGT ATCCGACCTTCTT-3' primers.

Thermal asymmetric interlaced (TAIL) PCR

Thermal asymmetric interlaced (TAIL) PCR was carried out according to (Liu et al. 2012). Three primers specific to the left border of pROK2 T-DNA were designed according to the publication specifications (the two first primers with overlapping sequences, and the third one at least 50 bp downstream): LB1 (5'-ATTTTGCCGATTTTCGGAA CCACC-3'), LB2 (5'-ACCATCAAACAGGATTTTCGC CTGCT -3'), and LB3 (5'-CCGTCTCACTGGTGAAAA GAAAAACC -3') and the same degenerative primers AD1 (5'-NTCGASTWTSGWGTT-3'), AD2 (5'-NGTCGASWGANAWGAA -3') and AD3 (5'-WGTGNAGWANCANAGA -3') have been used for all three reactions. Amplicons from the second reaction were extracted from a 2% w/v agarose gel, and sent for Sanger sequencing to LGC Genomics (Ireland). The resulting sequences were aligned with corresponding regions of the *Arabidopsis thaliana* genome (TAIR10.1) from the NCBI database.

Cas9-directed mutagenesis of *Arabidopsis thaliana* Col-0

Cas9-directed mutagenesis was performed via the transformation of *A. thaliana* with a novel p3-Cas9-mcherry plasmid vector constructed in the SpillaneLab (Plasmid Map and Sequence in Supplementary Information). Briefly, the vector was constructed from the pORE03 backbone base (Coutu et al. 2007). First, a *BsaI* site from the Bar resistance gene was removed by converting A to G in the recognition site, conserving the encoded arginine residue; this was performed by *BsaI* and *HpaI* digestion

followed by ligation of annealed oligos for sequence replacement. The backbone was then digested with *EcoRI* and *SphI* and ligated to the corresponding pHEE401 (Wang et al. 2015) fragment (a kind gift from Dr. Qi-Jun Chen's lab, China Agricultural University, Beijing; Addgene plasmid #71,286; <http://n2t.net/addgene:71286>; RRID:Addgene_71286). A positive selectable marker was then inserted between the *NotI* and *SpeI* sites in the form of an *At2S3* (seed specific) promoter-driven mCherry gene block synthesized by Integrated DNA Technology (Leuven, Belgium), according to the protocol previously described (Gao et al. 2016).

The double guide system for Cas9-directed mutagenesis of *At4g01310* was designed according to pre-established protocol (Xing et al. 2014) to remove a 1067 bp fragment from the gDNA sequence (Fig. 1a). Both guides were designed using the CRISPR-P tool (Lei et al. 2014) and the obtained double pair of primers were used to amplify the double guide promoter cassette from the vector pCBC-DT1T2 (gift from Qi-Jun Chen, Addgene plasmid #50,590), as described by Xing et al. (2014):

- DT1-BsF: 5'-ATATATGGTCTCGATTGCAGCACA GCGCGATAGTGGTT-3' and
- DT1-F0: 5'-TGCAGCACAGGCGCGATAGTGGTTTTA GAGCTAGAAATAGC-3' (guide 1)
- DT2-BsR: 5'-ATTATTGGTCTCGAAACCTTACCT CGAGAGGATTATCAA-3' and
- DT2-R0: 5'-AACCTTACCTCGAGAGGATTATCAATC TCTTAGTCGACTCTAC-3' (guide 2)

The obtained amplicon was cloned into the p3-Cas9-mCherry vector using the Golden Gate reaction with *BsaI* restriction as described previously (Weber et al. 2011) with some modifications: one cycle of 5 min at 32 °C and 5 min at 16 °C for over 5 h, followed by 5 min at 50 °C and 10 min at 80 °C in a Applied Biosystems Veriti 96-well thermal cycler (ThermoFisher Scientific, Paisley, UK).

The novel p3-Cas9-mcherry vector was used to transform *E. coli* DH α electrocompetent cells using electroporation. Cells were plated on LB agar with 50 μ g/ml kanamycin, and incubated overnight at 37 °C. The vector was purified from a positive colony saturated culture solution using a plasmid extraction kit (Biolone, Dublin, Ireland), and the Cas9 cassette sequence was confirmed by Sanger sequencing (LGC genomics, Berlin, Germany). Electrocompetent cells of *Agrobacterium tumefaciens* strain GV3101 were transformed with the sequenced vector by the same method, and inoculated onto LB agar plates with 50 μ g/ml kanamycin, 50 μ g/ml rifampicin and 100 μ g/ml gentamycin. Plates were incubated for two days at 28 °C.

Positive colonies were inoculated in LB broth with the same antibiotic concentrations for 2 days at 28 °C. Cells were then centrifuged and re-suspended in LB broth with 5% w/v sucrose and 0.02% v/v Silwett. This liquid culture was then used for *A. thaliana* flower dip method (Clough and Bent 1998), and seeds were harvested at the end of the plant life cycle.

Seeds were screened for transformants using the red fluorescence of the ERFP from the p3-Cas9-mcherry vector under green light, and positive T1 seedlings were grown on soil. Because no mutants were found within the T1

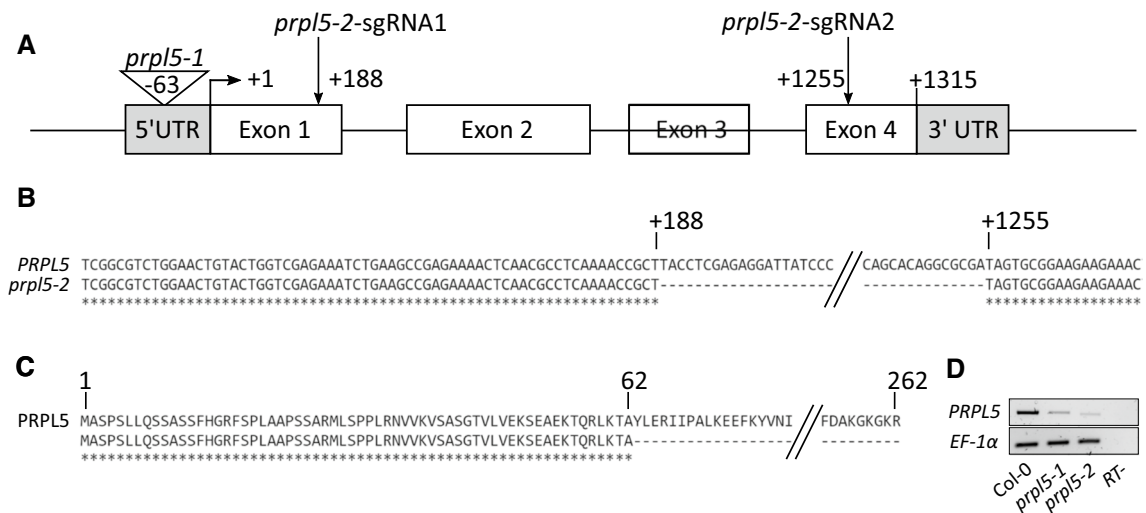


Fig. 1 Mutant alleles of *PRPL5* and expression data on mutant lines *prpl5-1* and *prpl5-2* used in this study. **A** Insertional mutant line *prpl5-1* and Cas9-generated mutant line *prpl5-2*. **B** Genomic sequence alignment between *PRPL5* WT sequence and *prpl5-*

2 mutant sequence validated by Sanger Sequencing. **C** Predicted amino-acid sequence of *PRPL5* aligned with the predicted amino-acid sequence of *PRPL5-2* mutant line. **D** RT-PCR of *PRPL5* expression in both *prpl5-1* and *prpl5-2*

generation, seeds were harvested from T1 lines, screened for ERFp signal, and positive seeds were grown on soil. T2 seedlings were screened for Cas9-induced mutation by PCR, and positive bands were sent for Sanger sequencing and aligned against corresponding regions of the *A. thaliana* genome to confirm the removal of the sequence of interest.

Cloning and transformation of *A. thaliana*

Genomic DNA sequences from *PRPL5* were amplified by Velocity DNA polymerase (BioLine, UK) using gateway-tailed primers and cloned first in pDONR221 and then in destination vector pB7YWG2 using the two-step gateway cloning system via BP and LR clonase reactions (Invitrogen, UK). Four different fragments were generated and cloned under the control of the 35S CamV promoter as fusion proteins with a C-terminal EYFP tag for fluorescence imaging: *PRPL5*, $\Delta_{233-262}$ *PRPL5*, Δ_{1-41} *PRPL5*, and $\Delta_{(1-41)+(233-262)}$ *PRPL5*.

A set of four gateway-tailed primers were used: two primers for the full *PRPL5* sequence (Forward 5'-attB1-ATG GCGTCTCCTTCGCTTC-3' and Reverse 5'-ATCTCTTTCCTTTTCCTTTAGCATCAAAG-attP1-3') and two for the N-ter and C-ter truncated sequence (Forward 5'-attB1-ATG GCGTCTGGAAGTACTGGTC-3' and Reverse 5'-ACC TGAAAGGCATTCCCATTAGAG-attP1-3'). One base was added to the reverse primers in 5' to keep *PRPL5* and *EYFP* in frame.

A. thaliana Col-0 lines were transformed by floral dip, as previously described. Resulting offspring were sprayed with 0.2 µg/ml of Basta to screen for transformants. Efficient transformation was verified by amplifying the YFP sequence by PCR using forward 5'–3' and reverse 5'–3' primers and transformants with good fluorescence intensity were crossed with the chloroplast reporter line pt-ck (Nelson et al. 2007). Small pieces (1 cm square) of leaf tissue from offspring plants were mounted on a microscopic slide in 5 µg/ml DAPI in PBS buffer and visualized with an Olympus BX51 epifluorescence microscope (Dublin, Ireland) with an UV source X-cite Series 120 Q (EXFO, Knightwood, UK). Images were captured with a Leica DFC7000 T camera (Leica microsystems, Ashbourne, Ireland). The same vectors and *A. thaliana* transformation method were used to transform *prpl5-1* and *prpl5-2* mutants for the complementation rescue experiment.

Sample preparation for transmission electron microscopy (TEM) analysis

Seeds were harvested at 4 days after pollination (DAP) from manually self-pollinated flowers from *prpl5-2* ± line and were fixed with a first solutions [2% v/v glutaraldehyde and 2% v/v paraformaldehyde in 0.1 M sodium cacodylate

buffer pH 7.2] followed by a second solution [1% w/v osmium tetroxide in 0.1 M sodium cacodylate buffer pH 7.2] according to the procedure from NUI Galway Centre for Imaging. The seeds were then progressively dehydrated with increasing concentrations of ethanol up to 100%, washed in acetone, and finally embedded in resin using the Agar Low Viscosity Resin kit (Agar Scientific, Stansted, UK) according to the manufacturer's protocol, and left for polymerisation at 65 °C for 48 h. Samples were cut using an ultramicrotome, survey sections of 500 nm width were cut using a glass knife, and stained with toluidine blue for microscope observation. From these, regions of interest were identified and trimmed to produce 70–90 nm sections using a diamond knife. Obtained sections were stained with uranyl acetate and lead citrate in the Leica EM AC20 automatic stainer (Leica microsystems, Ashbourne, Ireland) and allowed to air dry on a grid before visualization on a Hitachi 7500 Transmission electron microscope (Hitachi, Daresbury, UK).

Identification of *PRPL5* homolog sequences in Chlorophyta and Streptophyta

An initial search was performed by using the *PRPL5* protein sequence from *A. thaliana* as query for a BLASTX search in Chlorophyta and Streptophyta (Mount 2007). The identified sequences were compiled and aligned using MUSCLE (version 3.5, Edgar (2004)) for phylogeny construction. The phylogeny was established using PhyML (version 3.0, Guindon et al. (2010)), and the phylogenetic tree was built using TreeDyn (version 196, Chevenet et al. (2006)).

Results

PRPL5 is essential for seed development in *Arabidopsis thaliana*

In a forward genetic screen for seed abortion mutants, we observed a 23.5% seed abortion mutant phenotype in the T-DNA line SALK_015079 which was not segregating with the mutations on *AT3G59380* reported in the line by the Nottingham Arabidopsis Stock Centre (Fig. 2A and B). To identify the gene associated with the seed abortion phenotype, we used a TAIL-PCR approach on DNA extracted from a plant harboring the phenotype, which revealed the presence of a so far unreported pROK2 T-DNA insertion in the 5'UTR region of *AT4G01310* (Fig. 1A), which codes for the PLASTID RIBOSOMAL PROTEIN L5 (*PRPL5*) according to previous proteomic characterization (Zybailov et al. 2008; Ferro et al. 2010).

The genetic segregation of the insertion in *AT4G01310* (*PRPL5*) in the F1 offspring of a self-fertilized heterozygous parent followed a 1:2 ratio between genotyped wild-type

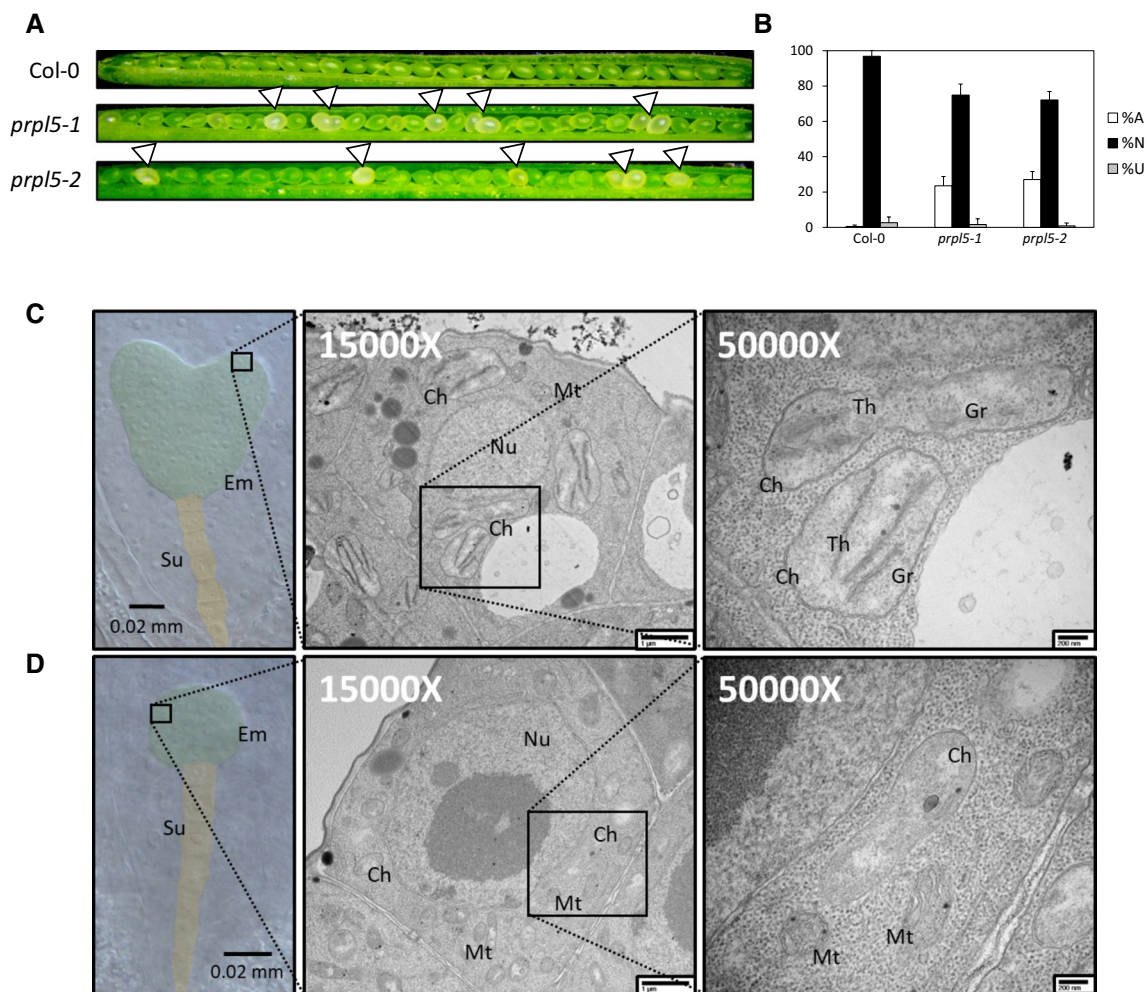


Fig. 2 Heterozygous mutant of *AT4G01310* leads to 25% seed abortion phenotype. Seed and plastid phenotype observed in both mutant lines in comparison to WT Col-0. **A** Developing seeds in siliques at 7 DAP. Aborting seeds are white and indicated by arrows. **B** Percentage of ANU (Aborted, Normal and Unfertilized) seeds for WT, *prp15-1* and *prp15-2* lines. **C** Green seed embryo from *prp15-2* at 4 DAP (heart stage) seen in false colors. The embryo has been highlighted in green while the suspensor has been highlighted in yellow. Chlo-

roplasts as fully developed as shown on TEM pictures aside, with presence of thylakoid and grana in the chloroplast matrix. **D** White seed embryo from *prp15-2* at 4 DAP (arrested at globular stage) seen in the same false colors as above. Chloroplasts are under-developed as shown on TEM pictures aside, with no thylakoid nor grana being observed in the plastid matrix. *Em* Embryo, *Su* Suspensor, *Ch* Chloroplast, *Nu* Nucleus, *Mt* Mitochondria, *Th* Thylakoid, *Gr* Granum

plants and heterozygous mutants (χ^2 test on 20 plants, p -value = 0.7903), with the total absence of any homozygous mutant offspring. The presence of the mutation in *PRPL5* correlated exclusively with the presence of the seed abortion mutant phenotype. To confirm the causality of the insertion on the phenotype, we performed a Cas9-directed mutagenesis on wild-type (WT) Col-0 line using the double guide targeting method (Xing et al. 2014) with a p3-Cas9-mcherry vector to generate a 1057 bp deletion in the *PRPL5* genomic sequence (Fig. 1A and B). Transformants were isolated from T2 generation seed by Enhanced Red Fluorescent protein (ERFP) fluorescence and the presence of a mutant allele of *PRPL5* was verified by Sanger sequencing across the deleted region. This verification further demonstrated

that the 1057 bp removal created a stop codon immediately after the 5' Cas9 cut (Fig. 1C). The offspring were then harvested and transgene-free lines were isolated by screening for non-fluorescent seeds. A 27.0% seed abortion phenotype was observed from this purified line, agreeing with the segregation ratio previously observed (Fig. 2A and B). Again, with this Cas9-generated *prp15* mutant line, no homozygous mutant could be isolated from the offspring and the presence of the deletion mutation in *PRPL5* followed a 1:2 distribution for WT and heterozygous mutants (χ^2 test on 60 plants, p -value = 0.7589) and correlated with the presence of the seed abortion phenotype. Since no mutants of *PRPL5* have so far been reported in the scientific literature, the two mutant alleles described in this study are hereafter named

prpl5-1 (SALK line) and *prpl5-2* (Cas9-mutated line). *PRPL5* mRNA expression was quantified by semi-quantitative RT-PCR (Fig. 1D) using a pair of primers spanning the locus for both *prpl5-1* and *prpl5-2* mutations, where any mutant allele mRNA from either *prpl5-1* or *prpl5-2* mutant lines would not amplify. As both of these mutant lines are heterozygous, we expected a decrease of *PRPL5* expression in both the *prpl5-1* and *prpl5-2* lines in comparison to *PRPL5* expression levels in wild-type Col-0, since one of the two *PRPL5* alleles in each heterozygous line was genotyped as wild type. The semi-quantitative RT-PCR results confirm that the heterozygous lines of *prpl5-1* and *prpl5-2* display reduced expression levels as expected from lines with only one wild-type copy.

Lack of *PRPL5* function causes post-globular embryo arrest

Seeds from siliques collected from self-pollinated *prpl5-2* heterozygous mutant plants were extracted at different time-points from 1 to 6 days after Pollination (DAP) and cleared. Compared to wild type, normal embryogenesis was observed in all developing seeds from the heterozygous mutant parent up to 3 DAP. After this timepoint, the embryos of 72.1% of the progeny seeds continue to develop normally (Fig. 2C). However, the other 27% of developing seeds remained white after this timepoint (identified as homozygous mutants) and displayed a post-globular stage embryo arrest phenotype (Fig. 2D). The remaining 0.9% of the ovules were unfertilized.

To determine whether the embryo abortion phenotype is associated with aberrant plastid development, progeny seeds from siliques obtained from self-pollinated *prpl5-2* heterozygous mutants were extracted at 4 DAP and processed for Transmission Electron Microscopy (TEM). Phenotypically normal plastids were observed in the normally developing embryos (green seeds), including the presence of fully developed thylakoids and grana (Fig. 2C). In contrast, while the plastid double envelope was still visible in post-globular arrested (homozygous mutant) embryos, the plastids were less than half the size of wild-type plastids and completely lacked any thylakoids or grana (Fig. 2D). Hence, we demonstrate that a homozygous mutation of *PRPL5* leads to defective plastid development causing embryo arrest at the globular stage and subsequent seed abortion.

The *PRPL5* N-terminal peptide sequence is necessary for plastid localization, while the C-terminal peptide sequence is not

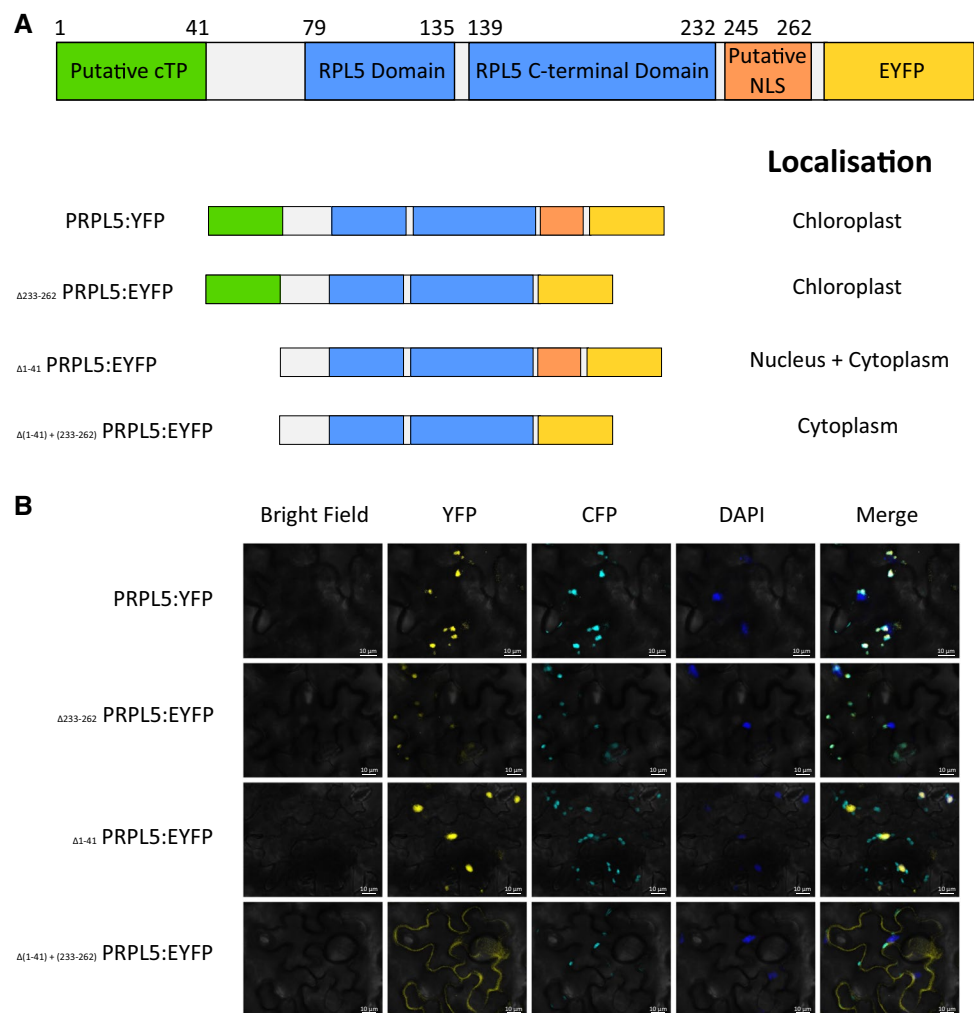
As the nuclear-encoded *PRPL5* gene is essential for plastid development, its protein product must be targeted to the plastid by anterograde signaling early during embryogenesis.

Hence, we sought to identify the molecular basis of its intracellular targeting. Bioinformatic analysis of the *PRPL5* peptide sequence with ChloroP (Emanuelsson et al. 1999) predicted amino acids 1 to 39 to form a chloroplast transit peptide (cTP) with relative certainty (Score 0.575). In contrast, PROSITE (Sigrist et al. 2002) and cNLS mapper predictor (Kosugi et al. 2009) identified amino acids 245–262 to form a bipartite nuclear localization signal with a middle level score of 3.7 for cNLS mapper (Fig. 3A). Interestingly, analysis of the Cryo-EM structure of the *Spinacea oleracea* plastid ribosome (Perez Boerema et al. 2018) indicates that the amino acids 1–41 at the N-terminus and from 233 onwards at the C-terminus sequences are absent from the protein once incorporated into the plastid ribosome (Fig. 3A). This suggests that the nascent *PRPL5* polypeptide contains multiple intracellular targeting sequences. To investigate these targeting sequences and determine their intracellular localisation functionality, we used the cleavage sites identified in *PRPL5* from *S. oleracea*, which are very close to the one in *A. thaliana*, to delimit both N-terminal and C-terminal sequences and to investigate their effect on *PRPL5* intracellular localisation.

To interrogate the intracellular localisation functionality of different *PRPL5* peptide regions, four constructs were generated from the *PRPL5* wild-type sequence and used to stably transform *Arabidopsis* Col-0 plants. The first construct consisted of a C-terminal fusion of *PRPL5* to *EYFP* (i.e., p35S:*PRPL5*:*EYFP*) and was used as a positive control for *PRPL5* protein localisation. The other three constructs were designed to lack either the N-terminal peptide sequence (i.e., p35S: Δ_{1-41} *PRPL5*:*EYFP*), the C-terminal peptide sequence (i.e., p35S: $\Delta_{233-262}$ *PRPL5*:*EYFP*), or both (i.e., p35S: $\Delta_{(1-41)+(233-262)}$ *PRPL5*:*EYFP*). These constructs were used to stably transform *A. thaliana* Col-0 and transformants with good fluorescence intensity were crossed with the chloroplast reporter line pt-ck (Nelson et al. 2007). To visualize intracellular localization, leaf tissue was mounted on microscopic slide with a 5 $\mu\text{g}\cdot\text{L}^{-1}$ DAPI solution for fluorescence imaging.

The positive control *PRPL5*:*EYFP* protein construct co-localized with chloroplasts, as expected for a nuclear-encoded plastid protein (Fig. 3A). Such co-localization with chloroplast also was observed with $\Delta_{233-262}$ *PRPL5*:*EYFP* lacking the C-terminal targeting sequence (Fig. 3B). However, the protein Δ_{1-41} *PRPL5*:*EYFP*, which lacks the N-terminal sequence, did not co-localize with chloroplasts but rather localized within the cytosol, as well as in the nucleus (Fig. 3C). Finally, the $\Delta_{(1-41)+(233-262)}$ *PRPL5*:*EYFP* construct lacking both N- and C-terminal peptide sequences localized exclusively in the cytosol (Fig. 3D). Overall, these results indicate that both predicted targeting sequences are functional although localization of *PRPL5* to the nucleus only occurs in the absence of the N-terminal cTP sequence.

Fig. 3 Subcellular localization of PRPL5:YFP protein constructs in *A. thaliana* leaf epidermal cells. Subcellular localization of four different PRPL5:YFP construct within *A. thaliana* leaf abaxial cells to interrogate the localization functionality of predicted N-ter and C-ter signaling peptides. **A** C-terminal fusion protein of PRPL5 with EYFP (Venus). Description of the localisation of each fusion protein: PRPL5:EYFP (Full protein positive control), $\Delta_{233-262}$ PRPL5:EYFP (C-terminal truncated protein), Δ_{1-41} PRPL5:EYFP (N-terminal truncated protein, and $\Delta_{(1-41)+(233-262)}$ PRPL5:EYFP (N-ter and C-ter truncated negative control). **B** EYFP visualization of protein localization. PRPL5:EYFP and $\Delta_{233-262}$ PRPL5:EYFP co-localize with chloroplast reporting signal, Δ_{1-41} PRPL5:EYFP co-localize with DAPI (nucleus), and $\Delta_{(1-41)+(233-262)}$ PRPL5:EYFP localizes only in the cytoplasm. Nucleus localisation is displayed using DAPI and chloroplasts localisation is displayed using a CFP construct inherited from the *A. thaliana* pt-ck reporter line. White bar represents 10 μm



The cTP of PRPL5 is essential for complementation of the *prpl5-1* and *prpl5-2* mutant phenotypes

The PRPL5 fusion and truncated protein constructs were used in complementation assays for the 25% seed abortion phenotype (observable in *prpl5-1* and *prpl5-2* heterozygotes) to confirm that PRPL5 is responsible for the observed abortion phenotype and also to interrogate the functions of the targeting peptides in relation to the seed abortion phenotype (Fig. 4). Both *prpl5-1* and *prpl5-2* heterozygous mutants were stably transformed with each of the four constructs by floral dipping and transformants were selected with Basta. The percentages of fertilized and unfertilized ovules and aborted and normal seeds were assessed for each transformant as previously reported to assess both fertility and viability (Duszynska et al. 2019). The expression of each transgene was also verified by both YFP fluorescence and RT-qPCR. Both the PRPL5:EYFP and $\Delta_{233-262}$ PRPL5:EYFP constructs were able to fully restore the WT phenotype in both of the heterozygous mutant lines, whereas the heterozygous mutants transformed with Δ_{1-41} PRPL5:EYFP

and $\Delta_{(1-41)+(233-262)}$ PRPL5:EYFP constructs still displayed 25% seed abortion (Fig. 4B) despite strong expression of the transgenes (Fig. 4C and D). Therefore, the constructs with the N-terminal deletion are unable to complement the *prpl5* loss-of-function alleles, as expected given their lack of plastid localisation. The genotyping of the T2 complemented generation further revealed the presence of homozygous mutants for both *prpl5-1* and *prpl5-2* complemented by PRPL5:EYFP and $\Delta_{233-262}$ PRPL5:EYFP, demonstrating the capability of both constructs to rescue PRPL5 function. Therefore, plastid localisation of PRPL5 with a cTP sequence is required for *A. thaliana* embryogenesis, while nuclear localisation is not required despite the NLS being functional.

PRPL5 transitioned from plastid-encoded to nuclear-encoded in the common ancestor of embryophytes

To gain evolutionary insights into the function of both N-terminal and C-terminal signaling peptides of PRPL5

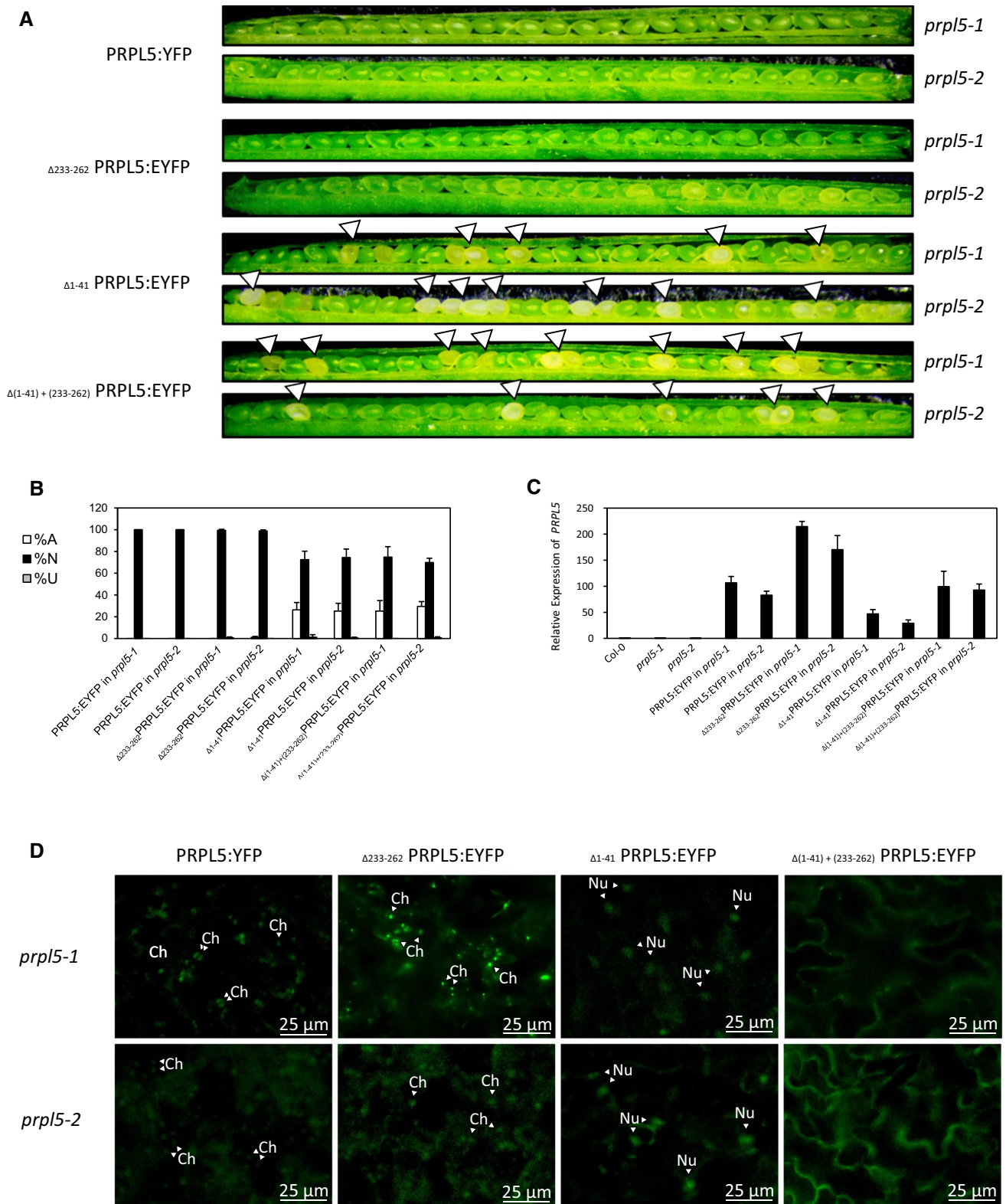


Fig. 4 Genetic complementation rescue experiment of *prpl5-1* and *prpl5-2*. Seed phenotype of mutant lines *prpl5-1* and *prpl5-2* rescued with different constructs of PRPL5:YFP harboring no, one, or both N-ter and C-ter signaling peptides. **A** Developing seeds in 7 DAP siliques from transformed *prpl5-1* and *prpl5-2* lines. **B** % of unfer-

tilized ovules (U), and normal and aborted seeds (N, A), for transformed *prpl5-1* and *prpl5-2* lines. **C** RT-qPCR of p35S:PRPL5:YFP in leaves of transformed *prpl5-1* and *prpl5-2* plants. **D** PRPL5:YFP fluorescence in rescued mutant lines. *Ch* Chloroplast, *Nu* Nucleus

we investigated the origin of PRPL5 through the evolution of Viridiplantae. From the comparison between PRPL5 sequences from Chlorophytes to spermatophytes, we found that the PRPL5 protein is exclusively nuclear-encoded in every sequenced species of the Embryophyta clade (Fig. 5). Both the N-terminal and C-terminal sequences of PRPL5 are well conserved in all seed plants (Spermatophyta) with circa 40% sequence identity for the N-terminal sequence, and circa 60% sequence identity for the C-terminal sequence. When compared to *A. thaliana*, the PRPL5 sequences of *Zea mays* and *Ananas comosus* were found to be the most distant with only 28% sequence identity to *A. thaliana* for the N-terminal sequence and 50% for the C-terminal, suggesting some divergence of PRPL5 sequence variation in monocots. The first and last 10 amino acids of the N-terminal sequence are the most conserved, while an RKK_LK_HHF_K_KG motif in the C-terminal sequence is also extremely well conserved across all analyzed sequences from Embryophyta.

All other groups from Chlorophyta and Charophyta (all Streptophyta species except land plants (Petersen et al. 2006)) have PRPL5 exclusively encoded in their plastid genomes, indicating that the gene underwent transfer to the nuclear genome in the common ancestor of Embryophytes (indicated with a blue star in Fig. 5). No conserved N-terminal nor C-terminal sequences comparable to those in Embryophyta can be detected in the PRPL5 sequence from any Chlorophyta or Charophyta species. The protein sequences of PRPL5 found in Lycophyta and Bryophyta both possess an N-terminal and C-terminal signaling peptide, but these are not well conserved comparative to the ones found in Spermatophyta species. We find only 22% identity for the N-terminal sequence from *Physcomitrium patens* when compared the one from *A. thaliana*, and 18% identity for *Selaginella moellendorffii*. The C-terminal sequence also harbors only 20% and 24% identity for *P. patens* and *S. moellendorffii*, respectively, in comparison to *A. thaliana*. In addition, both the N-terminal and C-terminal sequence tracts appear to be longer in both species in comparison to *A. thaliana* (53 and 54 amino acids for *P. patens* and *S. moellendorffii*, respectively, compared to 39 amino acids for Spermatophyta species), with the C-terminal section also lacking the Spermatophyta conserved motif. Despite these differences, ChloroP predicts N-terminal sequences as cTPs with a similar certainty as for the *A. thaliana* PRPL5 sequence (scoring at 0.505 for *S. moellendorffii*, 0.581 for *P. patens*). The C-terminal sequence is also predicted by cNLS mapper predictor as being a bipartite NLS in *S. moellendorffii* and *P. patens*, albeit with less certainty than for *A. thaliana* (scores of 2.0 for both). Thus, the transition of PRPL5 from being plastid-encoded to nuclear-encoded after the divergence of Embryophytes from Charophytes can be associated with the co-appearance of both plastid and nuclear localization signals.

Discussion

PRPL5 is required for plastid development

The bacterial homolog of *A. thaliana* PRPL5 (i.e., RPLE) has been reported as essential in *E. coli* (Shoji et al. 2011), but any requirement of PRPL5 for plant function has not previously been determined. As previously observed with most essential PRPs, a lack of functional PRPL5 does not allow any embryo development past the globular stage and causes embryo cells to proliferate ectopically while cotyledon initiation fails to occur. We demonstrate by TEM imaging that no thylakoids develop in plastids from either *prpl5-1* or *prpl5-2* homozygous mutants, consistent with the smaller and under-developed plastid phenotype reported in knockout mutants of PRPL21 (Yin et al. 2012). This plastid requirement for normal embryogenesis is also observed across different protein pathways. The knockout of the plastid Glycyl t-RNA transferase *EDD1* also leads to embryo failure, highlighting the importance of protein translation in plastids at such an early stage (Uwer et al. 1998). The same embryo phenotype can be observed with the knockout of *DLC* (Bellaoui et al. 2003) and the Stromal Processing Peptidase gene *SPP* (Trösch and Jarvis 2011) intervening in the cleavage of plastid transit peptides. More recently, two partially redundant nuclear-encoded chloroplast proteins for growth and fertility (genes *CGF1* and *CGF2*) have been reported as embryo-defective, as well as being required for normal female gametogenesis (Zhu et al. 2020). This underlines the importance of anterograde protein signaling for the functioning of chloroplasts and the role of chloroplast during early embryogenesis.

An explanation for the requirement of a well-functioning plastid at such an early stage of embryo development (prior to any photosynthetic activity) can be derived from the essentiality of plastid-derived lipid and starch biosynthesis pathways (Neuhaus and Emes 2000). One of the genes involved in such pathways is *accD* (which encodes a plastid acetyl-CoA Carboxylase and is essential for embryogenesis (Kode et al. 2005)), remains located within the plastid genome in *A. thaliana* while all the other genes related to the same pathways have already been transferred to the nuclear genome during evolution. The plastid genome harboring the only copy of *accD* in *A. thaliana* contrasts with other species (such as *Z. mays* (Bryant et al. 2011) and different species from the *Campanulaceae* lineage (Rousseau-Gueutin et al. 2013)), *accD* homologues have undergone transfer to the nuclear genome. In comparison to *A. thaliana*, impairment of the plastid translation machinery does not lead to embryo defect phenotypes in *Z. mays* but only to an impairment of the greening

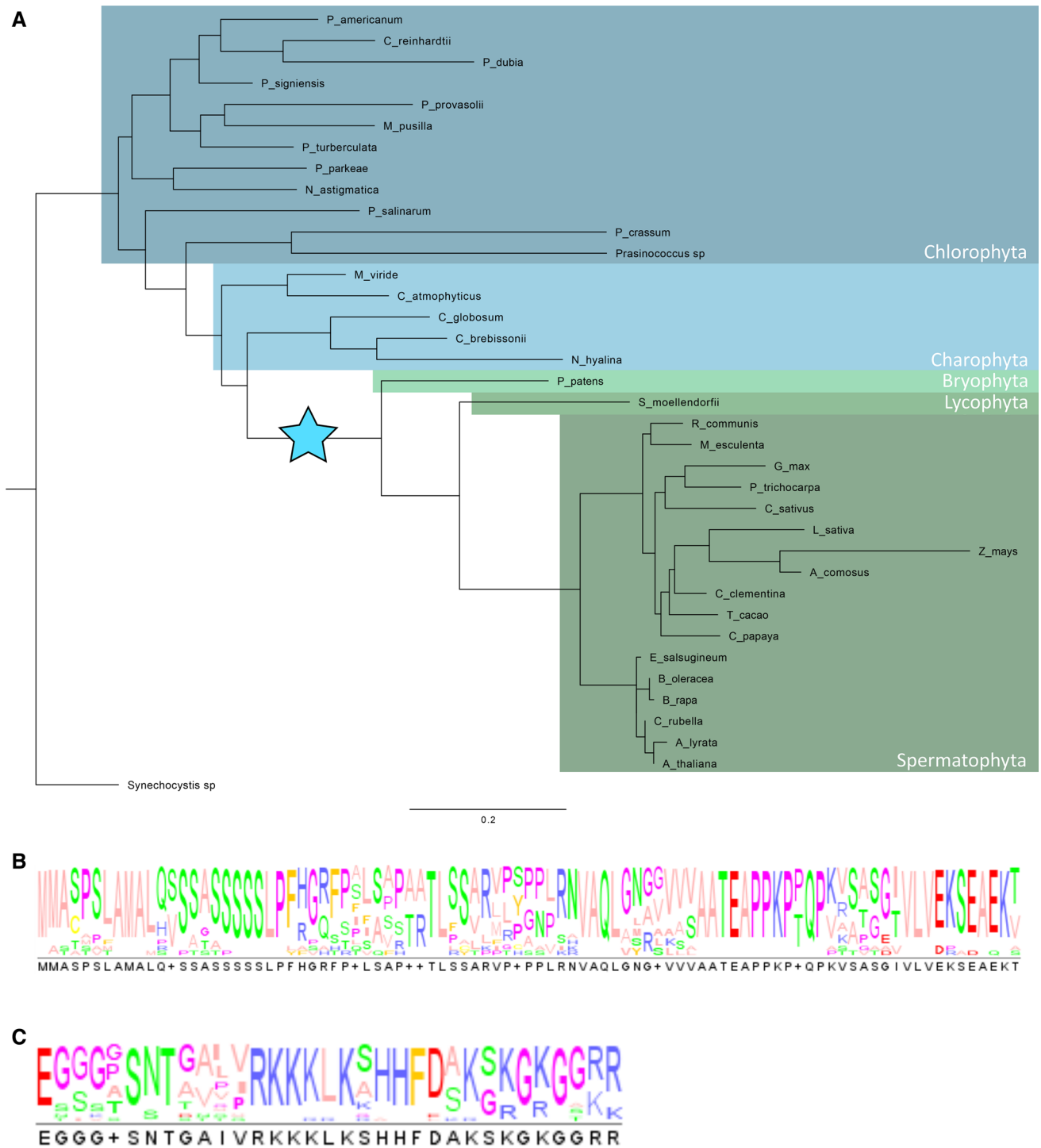


Fig. 5 Evolution of PRPL5 across *Chlorophyta* and *Embryophyta*. Study of PRPL5 molecular evolution in Viridiplantae and conservation of N-ter and C-ter signaling peptides across species **A** Phylogenetic tree of the PRPL5 sequence in Viridiplantae. The tree is rooted on the cyanobacteria species *Synechocystis sp.* (RPLE). Blue star

indicates the interval in which PRPL5 gene underwent transfer to the nuclear genome and corresponding loss from the plastid genome. **B** Consensus sequence of PRPL5 N-terminal signaling peptides among species displayed in the tree. **C** Consensus sequence of PRPL5 C-terminal signaling peptides among species displayed in the tree

process (Asakura and Barkan 2006; Bryant et al. 2011). This suggests that control of the lipid and starch biosynthesis pathways has been completely transferred over to the nucleus in these species and does not need plastid-related translation anymore to function, while in *A. thaliana* a part of this control is still shared between nucleus and plastid which jeopardizes its functionality in the event of plastid malfunction.

PRPL5 may play a core role in the cohesion of the plastid ribosome

It must be noted that, even though most PRPs are required for embryo development, there are also many PRP exceptions to this expectation. It is likely that some PRPs are more important than others for plastid ribosome activity depending on their position and functional role within the ribosome structure. As such, the necessity of PRPL5 can be assessed from investigation of the different interactions it can have within the whole quaternary protein complex. First, PRPL5 is known to form a heterodimer with PRPL11, this heterodimer binding to the 5S RNA to form one of the core elements of the large ribosome subunit (Steitz et al. 1988; Pelava et al. 2016). Second, the recent Cryo-EM structure of the spinach chloroplast ribosome shows that PRPL5 binds to RPL31, forming what is termed the central protuberance of the 50S ribosomal subunit. PRPL5 further is involved in a bridge between small and large ribosomal subunits via an interaction with PRPS13, an interaction strengthened by the association of the Ribosomal pY factor (Ahmed et al. 2016; Bieri et al. 2017; Perez Boerema et al. 2018). Despite not being the only bridge structure observed between both ribosomal subunits, PRPS13, however, appears to be required for plastid ribosome normal function, as mutations of *PRPS13* have also been reported as embryo-defective (Bryant et al. 2011; Lloyd and Meinke 2012). The maintenance of the large subunit central protuberance also seems to be required for ribosome normal activity, as *PRPL31* was also reported as essential for embryogenesis (Hsu et al. 2010). Overall, this suggests a central position for PRPL5 in the structural organization of the plastid ribosomal complex.

Roles of N-terminal and C-terminal peptide sequences in PRPL5

In this study we functionally demonstrate that the first 41 amino acids of PRPL5 act as a cTP (matching the predictions made by ChloroP). The plastid localization of the PRPL5 protein is also supported by mass spectrometry data from isolated chloroplasts (Kleffmann et al. 2004) and further reports added to the PPDB (Zybailov et al. 2008) and AT_CHLORO proteomic databases (Ferro et al. 2010). The N-terminal sequence of PRPL5 is well conserved among

land plants and seems to be exclusively responsible for PRPL5 localization within chloroplasts. The presence of the C-terminal peptide in PRPL5 leads to a localization of the protein within the nucleus, confirming PROSITE and cNLS mapper predictions. However, we report that such nuclear localization of PRPL5 only occurs when the N-terminal cTP is disrupted, suggesting that the cTP function is dominant over the NLS one. Since truncated version of PRPL5 lacking the C-terminal NLS sequence can still complement both mutant lines used in this study, it is unclear what role(s) the NLS peptide may play in PRPL5 function.

Comparisons with other nuclear-encoded PRPs also suggests that a C-terminal NLS can be predicted in the majority of PRPs. Only in PRPS1, -L4, -L17 and -L18 can no NLS be predicted. A recent study has demonstrated that the acquisition of a cTP on nascent plastid targeted proteins can usually be attributed to insertions or deletions in nearby genome sequences, followed by substitutions at a lower rate (Christian et al. 2020). Acquisition of a cTP by gene duplication is considered a less likely scenario, which could explain the weak alignment of cTP sequences from different nuclear-encoded PRPs within *A. thaliana* (Supplementary Fig. S5A). The same observation can be made with respect to the C-terminal NLS predicted in the majority of PRPs (Supplementary Fig. S5B). Hence, we can likely infer that cTPs and NLSs of the different nuclear-encoded PRPs were obtained from different origins.

However, in comparison to the importance of a cTP for the function of such proteins, which would explain its strong conservation across plant lineages (Fig. 5B), the high level of conservation of an NLS is puzzling (Fig. 5C). Such a high level of conservation would indicate a conservation of its function across plant lineages, but we could not identify any obvious phenotype in mutant lines rescued with a truncated version of PRPL5 lacking the C-terminal NLS under normal growth conditions. An interesting mechanism which could explain the role of PRPL5 C-terminal NLS would be the relocation of protein in the nucleus to perform a different function under stress conditions, possibly to be recruited by RNA polymerases to maintain genome integrity. This would be possible without the intervention of alternative splicing or post translational modifications, using a mechanism which has been named moonlighting and which uses close contacts between organelles and nucleus to allow such a transfer (Foyer et al. 2020; Krupinska et al. 2020). So far, PRPL5 has been identified in only one crude nuclear lamina protein fraction isolated from *A. thaliana* leaf-derived protoplast (Sakamoto and Takagi 2013) which could correlate with a nuclear relocation under particular stress conditions. Protoplasts indeed harbor an atypical and somewhat artificial cellular environment as cells are disconnected from their usual tissue. The process of protoplast isolation has also been reported to induce an oxidative burst and the activation

of oxidative stress responses genes, with an intensity varying between plant species (Papadakis and Roubelakis-Angelakis 1999).

Other PRPs have also been detected in nuclear environments in published nuclear proteomes. For instance, Bae et al. (2003) report the detection of PRPS5 and of a protein identified as a homolog of PRPL21 within a whole leaf tissue nuclear proteins extract. Both proteins were, however, identified as less present in the nuclear environment after application of cold stress. Similarly, Goto et al. (2019) report the presence of PRPS5, -S17 and -L21 in the proteome extracted from cultured cells nuclei, while Sakamoto and Takagi (2013) reports the presence of 24 PRPs in the proteome of protoplast nuclei in addition to PRPL5, namely PRPS1, -S5, -S9, -S13, -S17, -S20, -L1, -L3, -L4, -L6, -L9, -L10, -L11, -L13, -L15, -L17, -L18, -L21, -L24, -L27, -L28, -L29, -L31, and -L35. Such findings may link plastid protein relocation to the nucleus in the particular case of intense stress conditions and might explain the reported impact of some PRPs mutations on plant development only in stressful conditions, such as for PRPL33 (Rogalski et al. 2008). Hence, we could consider that PRPL5 could relocate in the nucleus under such conditions. However, any function of PRPL5 in the nuclear compartment is yet to be determined.

Conclusions

We demonstrate in this study that a protein of the central protuberance of the plastid 50S ribosomal subunit, namely PRPL5, is required for embryogenesis past the globular stage in *A. thaliana* indicating that PRPL5 is critical for the function of the plastid ribosome, and hence for translation. We further demonstrate that the N-terminal and C-terminal ends of the PRPL5 protein function, respectively, as a cTP and NLS, and further elucidate that the cTP is critical for protein function, while the NLS of PRPL5 is not. Despite its functionality as an NLS, the functional role and the conditions upon which this NLS signal is relevant to plant development and growth remains to be determined. The fact that this NLS signal is well conserved in all of its land plant homologues (especially in the seed plants) suggests some functional significance. Overall, our study identifies an essential role for the plastid 50S ribosomal subunit PRPL5 in embryogenesis and defines the functional cTP of the protein, while raising questions regarding the functional role of the predicted NLSs present in most nuclear-encoded plastid ribosomal proteins.

Supplementary Information The online version contains supplementary material available at <https://doi.org/10.1007/s00497-022-00440-9>.

Acknowledgements We thank Dr. Qi-Jun Chen's lab, China Agricultural University for the vector pHEE401 fragment, and acknowledge the support and facilities of the Microscopy Core Facility at the National University of Ireland Galway.

Funding Open Access funding provided by the IREL Consortium. This work was supported by a Science Foundation Ireland Principal Investigator Grant (13/IA/1820) to CS, and an Irish Research Council (IRC) PhD Fellowship Award to GD (GOIPG/2017/1219).

Availability of data and materials None.

Open Access This article is licensed under a Creative Commons Attribution 4.0 International License, which permits use, sharing, adaptation, distribution and reproduction in any medium or format, as long as you give appropriate credit to the original author(s) and the source, provide a link to the Creative Commons licence, and indicate if changes were made. The images or other third party material in this article are included in the article's Creative Commons licence, unless indicated otherwise in a credit line to the material. If material is not included in the article's Creative Commons licence and your intended use is not permitted by statutory regulation or exceeds the permitted use, you will need to obtain permission directly from the copyright holder. To view a copy of this licence, visit <http://creativecommons.org/licenses/by/4.0/>.

References

- Ahmed T, Yin Z, Bhushan S (2016) Cryo-EM structure of the large subunit of the spinach chloroplast ribosome. *Sci Rep* 6(1):35793. <https://doi.org/10.1038/srep35793>
- Allen JF (2018) Translating photosynthesis. *Nature Plants* 4(4):199–200. <https://doi.org/10.1038/s41477-018-0132-y>
- Asakura Y, Barkan A (2006) Arabidopsis orthologs of maize chloroplast splicing factors promote splicing of orthologous and species-specific group II introns. *Plant Physiol* 142(4):1656–1663. <https://doi.org/10.1104/pp.106.088096>
- Bae MS, Cho EJ, Choi E-Y, Park OK (2003) Analysis of the Arabidopsis nuclear proteome and its response to cold stress. *Plant J* 36(5):652–663. <https://doi.org/10.1046/j.1365-3113X.2003.01907.x>
- Bellaoui M, Keddie JS, Gruissem W (2003) DCL is a plant-specific protein required for plastid ribosomal RNA processing and embryo development. *Plant Mol Biol* 53(4):531–543. <https://doi.org/10.1023/B:PLAN.0000019061.79773.06>
- Bieri P, Leibundgut M, Saurer M, Boehringer D, Ban N (2017) The complete structure of the chloroplast 70S ribosome in complex with translation factor pY. *EMBO J* 36(4):475–486. <https://doi.org/10.15252/embj.201695959>
- Bobik K, Fernandez JC, Hardin SR, Ernest B, Ganusova EE, Staton Margaret E, Burch-Smith TM (2018) The essential chloroplast ribosomal protein uL15c interacts with the chloroplast RNA helicase ISE2 and affects intercellular trafficking through plasmodesmata. *New Phytologist*. <https://doi.org/10.1111/nph.15427>
- Boyes DC, Zayed AM, Ascenzi R, McCaskill AJ, Hoffman NE, Davis KR, Görlach J (2001) Growth stage-based phenotypic analysis of Arabidopsis: a model for high throughput functional genomics in plants. *Plant Cell* 13(7):1499–1510. <https://doi.org/10.1105/TPC.010011>
- Bräutigam K, Ditzel L, Pfannschmidt T (2007) Plastid-nucleus communication: anterograde and retrograde signalling in the development and function of plastids. In: Bock R (ed) *Cell and molecular*

- biology of plastids. Topics in current genetics. Springer, Berlin, Heidelberg, pp 409–455
- Bryant N, Lloyd J, Sweeney C, Myouga F, Meinke D (2011) Identification of nuclear genes encoding chloroplast-localized proteins required for embryo development in arabidopsis. *Plant Physiol* 155(4):1678–1689. <https://doi.org/10.1104/pp.110.168120>
- Chevenet F, Brun C, Bañuls A-L, Jacq B, Christen R (2006) TreeDyn: towards dynamic graphics and annotations for analyses of trees. *BMC Bioinform* 7(1):439. <https://doi.org/10.1186/1471-2105-7-439>
- Christian RW, Hewitt SL, Nelson G, Roalson EH, Dhingra A (2020) Plastid transit peptides—where do they come from and where do they all belong? Multi-genome and pan-genomic assessment of chloroplast transit peptide evolution. *PeerJ* 8:e9772. <https://doi.org/10.7717/peerj.9772>
- Clough SJ, Bent AF (1998) Floral dip: a simplified method for *Agrobacterium*-mediated transformation of *Arabidopsis thaliana*. *Plant J* 16(6):735–743. <https://doi.org/10.1046/j.1365-313x.1998.00343.x>
- Coutu C, Brandle J, Brown D, Brown K, Miki B, Simmonds J, Hegedus DD (2007) pORE: a modular binary vector series suited for both monocot and dicot plant transformation. *Transgenic Res* 16(6):771–781. <https://doi.org/10.1007/s11248-007-9066-2>
- Duszynska D, Vilhjalmsón B, Castillo Bravo R, Swamidatta S, Juenger TE, Donoghue MTA, Comte A, Nordborg M, Sharbel TF, Brychkova G, McKeown PC, Spillane C (2019) Transgenerational effects of inter-ploidy cross direction on reproduction and F2 seed development of *Arabidopsis thaliana* F1 hybrid triploids. *Plant Reproduct* 32(3):275–289. <https://doi.org/10.1007/s00497-019-00369-6>
- Edgar RC (2004) Muscle: multiple sequence alignment with high accuracy and high throughput. *Nucleic Acids Res* 32(5):1792–1797. <https://doi.org/10.1093/nar/gkh340>
- Emanuelsson O, Nielsen H, Heijne GV (1999) ChloroP, a neural network-based method for predicting chloroplast transit peptides and their cleavage sites. *Protein Sci* 8(5):978–984. <https://doi.org/10.1110/ps.8.5.978>
- Ferro M, Briugière S, Salvi D, Seigneurin-Berny D, Court M, Moyet L, Ramus C, Miras S, Mellal M, Le Gall S, Kieffer-Jaquinod S, Bruley C, Garin J, Joyard J, Masselon C, Rolland N (2010) AT_CHLORO, a comprehensive chloroplast proteome database with subplastidial localization and curated information on envelope proteins. *Molec Cell Proteom* 9(6):1063–1084. <https://doi.org/10.1074/mcp.M900325-MCP200>
- Fleischmann TT, Scharff LB, Alkatib S, Hasdorf S, Schöttler MA, Bock R (2011) Nonessential plastid-encoded ribosomal proteins in tobacco: a developmental role for plastid translation and implications for reductive genome evolution. *Plant Cell* 23(9):3137–3155. <https://doi.org/10.1105/tpc.111.088906>
- Foyer CH, Baker A, Wright M, Sparkes IA, Mhamdi A, Schippers JHM, Van Breusegem F (2020) On the move: redox-dependent protein relocation in plants. *J Exp Bot* 71(2):620–631. <https://doi.org/10.1093/jxb/erz330>
- Gao X, Chen J, Dai X, Zhang D, Zhao Y (2016) An Effective strategy for reliably isolating heritable and cas9-free arabidopsis mutants generated by CRISPR/Cas9-mediated genome editing. *Plant Physiol* 171(3):1794–1800. <https://doi.org/10.1104/pp.16.00663>
- Goto C, Hashizume S, Fukao Y, Hara-Nishimura I, Tamura K (2019) Comprehensive nuclear proteome of *Arabidopsis* obtained by sequential extraction. *Nucleus* 10(S12):81–92. <https://doi.org/10.1080/19491034.2019.1603093>
- Guindon S, Dufayard J-F, Lefort V, Anisimova M, Hordijk W, Gascuel O (2010) New algorithms and methods to estimate maximum-likelihood phylogenies: assessing the performance of PhyML 3.0. *System Biol* 59(3):307–321. <https://doi.org/10.1093/sysbio/syq010>
- Hsu SC, Belmonte FM, Harada J, Inoue K (2010) Indispensable roles of plastids in *Arabidopsis thaliana* embryogenesis. *Curr Genom* 11(5):338–349. <https://doi.org/10.2174/138920210791616716>
- Jiang T, Zhang J, Rong L, Feng Y, Wang Q, Song Q, Zhang L, Ouyang M (2018) ECD1 functions as an RNA-editing trans-factor of rps14-149 in plastids and is required for early chloroplast development in seedlings. *J Exp Bot* 69(12):3037–3051. <https://doi.org/10.1093/jxb/ery139>
- Kishino H, Miyata T, Hasegawa M (1990) Maximum likelihood inference of protein phylogeny and the origin of chloroplasts. *J Mol Evol* 31(2):151–160. <https://doi.org/10.1007/BF02109483>
- Kleffmann T, Russenberger D, Av Z, Christopher W, Sjölander K, Gruissem W, Baginsky S (2004) The *Arabidopsis thaliana* chloroplast proteome reveals pathway abundance and novel protein functions. *Curr Biol* 14(5):354–362. <https://doi.org/10.1016/j.cub.2004.02.039>
- Kode V, Mudd EA, Iamtham S, Day A (2005) The tobacco plastid accD gene is essential and is required for leaf development. *Plant J* 44(2):237–244. <https://doi.org/10.1111/j.1365-313X.2005.02533.x>
- Kosugi S, Hasebe M, Tomita M, Yanagawa H (2009) Systematic identification of cell cycle-dependent yeast nucleocytoplasmic shuttling proteins by prediction of composite motifs. *Proc Natl Acad Sci* 106(25):10171–10176. <https://doi.org/10.1073/pnas.0900604106>
- Krupinska K, Blanco NE, Oetke S, Zottini M (2020) Genome communication in plants mediated by organelle–nucleus-located proteins. *Philosoph Transact Royal Soc B Biol Sci* 375(1801):20190397. <https://doi.org/10.1098/rstb.2019.0397>
- Lei Y, Lu L, Liu H-Y, Li S, Xing F, Chen L-L (2014) CRISPR-P: a web tool for synthetic single-guide RNA design of CRISPR-system in plants. *Mol Plant* 7(9):1494–1496. <https://doi.org/10.1093/mp/ssu044>
- Liu S, Yeh C-T, Tang HM, Nettleton D, Schnable PS (2012) Gene mapping via bulked segregant RNA-Seq (BSR-Seq). *PLoS One* 7(5):e36406. <https://doi.org/10.1371/journal.pone.0036406>
- Lloyd J, Meinke D (2012) A Comprehensive dataset of genes with a loss-of-function mutant phenotype in arabidopsis. *Plant Physiol* 158(3):1115–1129. <https://doi.org/10.1104/pp.111.192393>
- Martin W, Rujan T, Richly E, Hansen A, Cornelsen S, Lins T, Leister D, Stoebe B, Hasegawa M, Penny D (2002) Evolutionary analysis of *Arabidopsis*, cyanobacterial, and chloroplast genomes reveals plastid phylogeny and thousands of cyanobacterial genes in the nucleus. *Proc Natl Acad Sci* 99(19):12246–12251. <https://doi.org/10.1073/pnas.182432999>
- McFadden GI (2014) Origin and evolution of plastids and photosynthesis in eukaryotes. *Cold Spring Harb Perspect Biol* 6(4):a016105. <https://doi.org/10.1101/cshperspect.a016105>
- Moreira D, Guyader HL, Philippe H (2000) The origin of red algae and the evolution of chloroplasts. *Nature* 405(6782):69–72. <https://doi.org/10.1038/35011054>
- Morita-Yamamuro C, Tsutsui T, Tanaka A, Yamaguchi J (2004) Knock-out of the plastid ribosomal protein S21 causes impaired photosynthesis and sugar-response during germination and seedling development in *Arabidopsis thaliana*. *Plant Cell Physiol* 45(6):781–788. <https://doi.org/10.1093/pcp/pch093>
- Mount DW (2007) Using the basic local alignment search tool (BLAST). *Cold Spring Harbor Protocols*. <https://doi.org/10.1101/pdb.top17>
- Muralla R, Lloyd J, Meinke D (2011) Molecular foundations of reproductive lethality in *Arabidopsis thaliana*. *PLoS ONE* 6(12):e28398. <https://doi.org/10.1371/journal.pone.0028398>

- Murashige T, Skoog F (1962) A Revised Medium for Rapid Growth and Bio Assays with Tobacco Tissue Cultures. *Plant Physiol* 15:473–497
- Nadine T, Magdalena W, Wolfram T, Eugenia M (2012) The plastid-specific ribosomal proteins of *Arabidopsis thaliana* can be divided into non-essential proteins and genuine ribosomal proteins. *Plant J* 69(2):302–316. <https://doi.org/10.1111/j.1365-313X.2011.04791.x>
- Nelson BK, Cai X, Nebenführ A (2007) A multicolored set of in vivo organelle markers for co-localization studies in *Arabidopsis* and other plants. *Plant J* 51(6):1126–1136. <https://doi.org/10.1111/j.1365-313X.2007.03212.x>
- Neuhaus HE, Emes MJ (2000) Nonphotosynthetic metabolism in plastids. *Annu Rev Plant Physiol Plant Mol Biol* 51(1):111–140. <https://doi.org/10.1146/annurev.arplant.51.1.111>
- Nowack ECM, Weber APM (2018) Genomics-informed insights into endosymbiotic organelle evolution in photosynthetic eukaryotes. *Annu Rev Plant Biol* 69(1):51–84. <https://doi.org/10.1146/annurev-arplant-042817-040209>
- Papadakis AK, Roubelakis-Angelakis KA (1999) The generation of active oxygen species differs in tobacco and grapevine mesophyll protoplasts. *Plant Physiol* 121(1):197–206. <https://doi.org/10.1104/pp.121.1.197>
- Pelava A, Schneider C, Watkins NJ (2016) The importance of ribosome production, and the 5S RNP–MDM2 pathway, in health and disease. *Biochem Soc Trans* 44(4):1086–1090. <https://doi.org/10.1042/BST20160106>
- Perez Boerema A, Aibara S, Paul B, Tobiasson V, Kimanius D, Forsberg BO, Wallden K, Lindahl E, Amunts A (2018) Structure of the chloroplast ribosome with chl-RRF and hibernation-promoting factor. *Nature Plants* 4(4):212–217. <https://doi.org/10.1038/s41477-018-0129-6>
- Pesaresi P, Masiero S, Eubel H, Braun H-P, Bhushan S, Glaser E, Salamini F, Leister D (2006) Nuclear photosynthetic gene expression is synergistically modulated by rates of protein synthesis in chloroplasts and mitochondria. *Plant Cell* 18(4):970–991. <https://doi.org/10.1105/tpc.105.039073>
- Petersen J, Teich R, Becker B, Cerff R, Brinkmann H (2006) The GapA/B gene duplication marks the origin of streptophyta (Charophytes and land plants). *Mol Biol Evol* 23(6):1109–1118. <https://doi.org/10.1093/molbev/msj123>
- Rogalski M, Ruf S, Bock R (2006) Tobacco plastid ribosomal protein S18 is essential for cell survival. *Nucleic Acids Res* 34(16):4537–4545. <https://doi.org/10.1093/nar/gkl634>
- Rogalski M, Schöttler MA, Thiele W, Schulze WX, Bock R (2008) Rpl33, a nonessential plastid-encoded ribosomal protein in tobacco, is required under cold stress conditions. *Plant Cell* 20(8):2221–2237. <https://doi.org/10.1105/tpc.108.060392>
- Romani I, Tadani L, Rossi F, Masiero S, Pribil M, Jahns P, Kater M, Leister D, Pesaresi P (2012) Versatile roles of *Arabidopsis* plastid ribosomal proteins in plant growth and development. *Plant J* 72(6):922–934. <https://doi.org/10.1111/tpj.12000>
- Rousseau-Gueutin M, Huang X, Higginson E, Ayliffe M, Day A, Timmis JN (2013) Potential functional replacement of the plastidic Acetyl-CoA carboxylase subunit (accD) gene by recent transfers to the nucleus in some angiosperm lineages. *Plant Physiol* 161(4):1918–1929. <https://doi.org/10.1104/pp.113.214528>
- Sakamoto Y, Takagi S (2013) LITTLE NUCLEI 1 and 4 regulate nuclear morphology in *Arabidopsis thaliana*. *Plant Cell Physiol* 54(4):622–633. <https://doi.org/10.1093/pcp/pct031>
- Shoji S, Dambacher CM, Shajani Z, Williamson JR, Schultz PG (2011) Systematic chromosomal deletion of bacterial ribosomal protein genes. *J Mol Biol* 413(4):751–761. <https://doi.org/10.1016/j.jmb.2011.09.004>
- Sigrist CJA, Cerutti L, Hulo N, Gattiker A, Falquet L, Pagni M, Bairoch A, Bucher P (2002) PROSITE: A documented database using patterns and profiles as motif descriptors. *Brief Bioinform* 3(3):265–274. <https://doi.org/10.1093/bib/3.3.265>
- Steitz JA, Berg C, Hendrick JP, La Branche-Chabot H, Metspalu A, Rinke J, Yario T (1988) A 5S rRNA/L5 complex is a precursor to ribosome assembly in mammalian cells. *J Cell Biol* 106(3):545–556. <https://doi.org/10.1083/jcb.106.3.545>
- Stiller JW (2007) Plastid endosymbiosis, genome evolution and the origin of green plants. *Trends Plant Sci* 12(9):391–396. <https://doi.org/10.1016/j.tplants.2007.08.002>
- Trösch R, Jarvis P (2011) The stromal processing peptidase of chloroplasts is essential in *Arabidopsis*, with knockout mutations causing embryo arrest after the 16-Cell Stage. *PLoS ONE* 6(8):e23039. <https://doi.org/10.1371/journal.pone.0023039>
- Uwer U, Willmitzer L, Altmann T (1998) Inactivation of a Glycyl-tRNA synthetase leads to an arrest in plant embryo development. *Plant Cell* 10(8):1277–1294. <https://doi.org/10.1105/tpc.10.8.1277>
- Wang H, Wang J, Jiang J, Chen S, Guan Z, Liao Y, Chen F (2014) Reference genes for normalizing transcription in diploid and tetraploid *Arabidopsis*. *Sci Rep* 4(1):6781. <https://doi.org/10.1038/srep06781>
- Wang Z-P, Xing H-L, Dong L, Zhang H-Y, Han C-Y, Wang X-C, Chen Q-J (2015) Egg cell-specific promoter-controlled CRISPR/Cas9 efficiently generates homozygous mutants for multiple target genes in *Arabidopsis* in a single generation. *Genome Biol* 16:144. <https://doi.org/10.1186/s13059-015-0715-0>
- Weber E, Engler C, Gruetzner R, Werner S, Marillonnet S (2011) A modular cloning system for standardized assembly of multigene constructs. *PLoS ONE* 6(2):e16765. <https://doi.org/10.1371/journal.pone.0016765>
- Woo HR, Chang-Hyo G, Joo-Hyuu P, Teyssendier dISB, Jin-Hee K, Youn-II P, Gil NH (2002) Extended leaf longevity in the ore4-1 mutant of *Arabidopsis* with a reduced expression of a plastid ribosomal protein gene. *Plant J* 31(3):331–340. <https://doi.org/10.1046/j.1365-313X.2002.01355.x>
- Xing H-L, Dong L, Wang Z-P, Zhang H-Y, Han C-Y, Liu B, Wang X-C, Chen Q-J (2014) A CRISPR/Cas9 toolkit for multiplex genome editing in plants. *BMC Plant Biol* 14:327. <https://doi.org/10.1186/s12870-014-0327-y>
- Yamaguchi K, Subramanian AR (2000) The plastid ribosomal proteins identification of all the proteins in the 50 s subunit of an organelle ribosome (Chloroplast). *J Biol Chem* 275(37):28466–28482. <https://doi.org/10.1074/jbc.M005012200>
- Yin T, Pan G, Liu H, Wu J, Li Y, Zhao Z, Fu T, Zhou Y (2012) The chloroplast ribosomal protein L21 gene is essential for plastid development and embryogenesis in *Arabidopsis*. *Planta* 235(5):907–921. <https://doi.org/10.1007/s00425-011-1547-0>
- Zhao P, Zhou X, Shen K, Liu Z, Cheng T, Liu D, Cheng Y, Peng X, Sun M-x (2019) Two-step maternal-to-zygotic transition with two-phase parental genome contributions. *Dev Cell* 49(6):882–893. e885. <https://doi.org/10.1016/j.devcel.2019.04.016>
- Zhu R-M, Chai S, Zhang Z-Z, Ma C-L, Zhang Y, Li S (2020) *Arabidopsis* chloroplast protein for growth and fertility1 (CGF1) and CGF2 are essential for chloroplast development and female gametogenesis. *BMC Plant Biol* 20(1):172. <https://doi.org/10.1186/s12870-020-02393-5>
- Zybailov B, Rutschow H, Friso G, Rudella A, Emanuelsson O, Sun Q, Wijk KJV (2008) Sorting signals, N-terminal modifications and abundance of the chloroplast proteome. *PLOS one* 3(4):e1994. <https://doi.org/10.1371/journal.pone.0001994>

Publisher's Note Springer Nature remains neutral with regard to jurisdictional claims in published maps and institutional affiliations.